



# N-(4-(di-*tert*-butyl[ $^{18}\text{F}$ ]fluorosilyl)benzyl)-2-hydroxy-N,N-dimethylethylammonium bromide ([ $^{18}\text{F}$ ]SiFAN $^+\text{Br}^-$ ): A novel lead compound for the development of hydrophilic SiFA-based prosthetic groups for $^{18}\text{F}$ -labeling

Alexey P. Kostikov<sup>a</sup>, Liuba Iovkova<sup>b</sup>, Joshua Chin<sup>a</sup>, Esther Schirmacher<sup>a</sup>, Björn Wängler<sup>c</sup>, Carmen Wängler<sup>c</sup>, Klaus Jurkschat<sup>b</sup>, Gonzalo Cosa<sup>d</sup>, Ralf Schirmacher<sup>a,\*</sup>

<sup>a</sup> McConnell Brain Imaging Centre, Montreal Neurological Institute, McGill University, 3801 University Street, Montreal, Quebec H3A3B4, Canada

<sup>b</sup> Lehrstuhl für Anorganische Chemie, Technische Universität Dortmund, Germany

<sup>c</sup> Department of Nuclear Medicine, Ludwig-Maximilians-University, Munich, Germany

<sup>d</sup> Department of Chemistry, McGill University, 801 Sherbrooke Street West, Montreal, QC H3A 2K6, Canada

## ARTICLE INFO

### Article history:

Received 28 September 2010

Received in revised form 26 October 2010

Accepted 27 October 2010

Available online 3 November 2010

### Keywords:

Isotopic exchange

Silicon-fluoride-acceptor (SiFA)

PET

Radiotracer

Fluorine-18

## ABSTRACT

$^{18}\text{F}$ -labeled compounds play a major role in the development of new *in vivo* imaging agents for Positron Emission Tomography (PET), a non invasive imaging modality depicting the biodistribution of radioactive compounds in humans. Recently we reported a new method for the introduction of fluorine-18 into a range of organic molecules exploiting the very fast  $^{18}\text{F}$ - $^{19}\text{F}$  isotope exchange of fluorosilanes (termed SiFA compounds). Here, we wish to report the labeling of the first charged SiFA molecule N-(4-(di-*tert*-butylfluorosilyl)benzyl)-2-hydroxy-N,N-dimethylethylammonium bromide (SiFAN $^+\text{Br}^-$ ) serving as a lead compound in the development of SiFA-based prosthetic groups of reduced lipophilicity for biomolecule labeling. Mild conditions for synthesis of [ $^{18}\text{F}$ ]SiFAN $^+\text{Br}^-$  and an easy purification procedure using simple C-18 solid phase cartridge have been developed yielding the [ $^{18}\text{F}$ ]SiFAN $^+\text{Br}^-$  in radiochemical yields of 34% (non-decay corrected) within 40 min. A series of kinetic experiments were performed that show high isotopic exchange rate constants. Low activation energy (15.7 kcal/mol) and a large preexponential factor ( $7.9 \times 10^{13} \text{ M}^{-1} \text{ s}^{-1}$ ) were calculated for the isotopic exchange reaction from a corresponding Arrhenius plot. For comparison, the  $^{18}\text{F}$ -fluorination of ethyleneglycol-di-*p*-tosylate via the formation of a carbon- $^{18}\text{F}$  bond showed a 1.3 kcal/mol higher activation energy and a much lower preexponential factor of  $2.9 \times 10^9 \text{ M}^{-1} \text{ s}^{-1}$ . Moderate hydrophilicity ( $\log D = 0.44$ ), stability in aqueous media at pH up to 7.4 and a high specific activity of [ $^{18}\text{F}$ ]SiFAN $^+\text{Br}^-$  (SA = 20.4 GBq/ $\mu\text{mol}$ , 0.55 Ci/ $\mu\text{mol}$ ) make this charged SiFA compound useful for the development of novel SiFA-based  $^{18}\text{F}$ -labeling synthons.

© 2010 Elsevier B.V. All rights reserved.

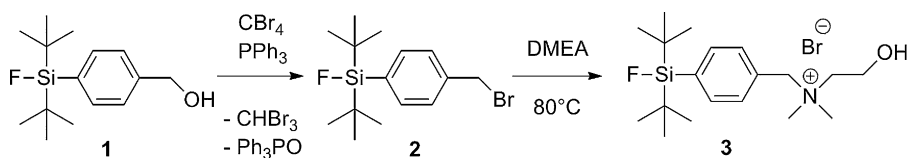
## 1. Introduction

Fluorine-18 is among the most widely used radioisotopes for Positron Emission Tomography (PET) due to its relatively long half-life (110 min) and low positron energy (635 keV) which allows for high-resolution imaging. Although many tracers have been synthesized and successfully used as PET imaging agents, only very few, most notably 2-[ $^{18}\text{F}$ ]fluoro-2-deoxy-D-glucose ([ $^{18}\text{F}$ ]FDG), have found widespread application in nuclear medicine [1]. This is mainly due to the fact that the nucleophilic reaction between azeotropically “dried”  $^{18}\text{F}^-$  and leaving group bearing precursors often requires harsh reaction conditions and thus time-consuming purification procedures, ultimately reducing the

overall radiochemical yields (RCYs) of the desired product. Novel mild methods for the labeling of small as well as larger biomolecules are thus highly sought after. The radiochemistry of PET radioisotopes and the particular chemistry of  $^{18}\text{F}$  and its role in PET tracer development have been the subject of many reviews [2]. Most notably, the  $^{18}\text{F}$ -labeling of more complex molecules such as peptides and proteins still predominantly depends on prosthetic  $^{18}\text{F}$ -labeling agents obtained via nucleophilic substitution employing the  $^{18}\text{F}^-$  anion. The prosthetic group (“ $^{18}\text{F}$ -labeling synthon”) is synthesized in advance and reacted with the biomolecule intended for PET imaging. Numerous  $^{18}\text{F}$ -labeled precursors have been reported in the literature predominantly utilizing click chemistry type reactions for the efficient conjugation to peptide or protein based PET imaging agents [2 g]. Recently, direct one-step  $^{18}\text{F}$ -labeling procedures for peptides taking advantage of either activated trimethylammonium leaving groups directly coupled to the N-terminus of the peptide or nucleophilic ring-opening of

\* Corresponding author. Tel.: +1 514 398 1624; fax: +1 514 398 8195.

E-mail address: [ralf.schirmacher@mcgill.ca](mailto:ralf.schirmacher@mcgill.ca) (R. Schirmacher).



**Scheme 1.** Synthesis of SiFAN<sup>+</sup>Br<sup>-</sup> starting from SiFA-benzyl alcohol (1) which was converted into the corresponding bromo compound 2 and reacted with N,N-dimethyl ethanolamine (DMEA) to yield SiFAN<sup>+</sup>Br<sup>-</sup> (3).

activated aziridines have proven to be feasible [3]. Although these approaches yield the <sup>18</sup>F-labeled peptides in one-step in high RCYs the final purification still required an HPLC.

Besides the common formation of a carbon-<sup>18</sup>F bond by nucleophilic substitution, only a few groups have investigated the potential of “non-conventional” phosphorous-, boron-, <sup>18</sup>F-aluminium chelates and silicon-<sup>18</sup>F-radiochemistry for the <sup>18</sup>F-labeling of organic compounds [4]. Our group has introduced a new <sup>18</sup>F-labeling method based on the <sup>18</sup>F-<sup>19</sup>F isotope exchange reaction using nanomolar amounts of *para* substituted di-*tert*-butylphenylfluorosilanes (SiFA-compounds; coined after silicon\_fluoride\_acceptor) at room temperature [5]. Isotopic exchange reactions involving a carbon-fluorine bond have already been applied in <sup>18</sup>F-labeling chemistry and it could be demonstrated that only products of low specific activity (SA) can be obtained hampering their use in PET tracer development [6]. In contrast to this, SiFA compounds can be obtained in high RCYs as well as high SA because of the efficiency of the isotopic exchange reaction. A great variety of SiFA compounds differing in substitution pattern at the benzene structure have been evaluated towards their amenability for isotopic exchange. Among those, *p*-(di-*t*-butyl[<sup>18</sup>F]fluorosilyl)benzaldehyde (SiFA-aldehyde) [5b] and *p*-(di-*t*-butyl[<sup>18</sup>F]fluorosilyl)benzene thiol (SiFA-SH) [5c] have been successfully applied as synthons for the labeling of peptides and proteins, respectively. Despite being successful labeling building blocks for proteins, yielding suitable *in vivo* images, a major drawback of these previously reported SiFA compounds for the labeling of peptides is their extremely high lipophilicity, accounting for a high accumulation of the radiotracer in the liver and unspecific binding to the target tissue. These findings were corroborated by Hoehne et al. who have independently developed a no-carrier-added silicon-based labeling technique using Si-F building blocks of similar structure [7]. It became apparent that the steric hindrance imparted by the *tert*-butyl groups of the SiFA building block is mandatory for maintaining a high stability of the Si-<sup>18</sup>F bond towards hydrolysis [5a]. At the same time, these bulky groups are responsible for the high lipophilicity of SiFA complicating their use as universally applicable <sup>18</sup>F-labeling synthons especially for compounds of lower molecular weight.

In order to reduce the overall lipophilicity of the SiFA-building block, and to find a chemical lead compound for the development of novel hydrophilic SiFA-based prosthetic groups, we introduced a positive chemical charge in the form of a tertiary ammonium salt into the SiFA molecule and investigated whether the isotope exchange reaction with <sup>18</sup>F<sup>-</sup> still occurs. We synthesized N-(4-(di-*tert*-butylfluorosilyl)benzyl)-2-hydroxy-N,N-dimethylethylammonium bromide (SiFAN<sup>+</sup>Br<sup>-</sup>), optimized the conditions for introducing <sup>18</sup>F<sup>-</sup> via isotopic exchange, measured the rate constants of the isotopic exchange at different temperatures and calculated the preexponential factor and activation energy for the <sup>18</sup>F-<sup>19</sup>F exchange from the corresponding Arrhenius plot. To further characterize SiFAN<sup>+</sup>Br<sup>-</sup>, we determined lipophilicity, stability in aqueous media at different pH and specific activity (SA), setting a compelling foundation for the future design of charged SiFA-based building blocks for the <sup>18</sup>F-labeling of biomolecules such as peptides and proteins.

## 2. Results and discussion

### 2.1. Synthetic aspects and molecular structure of the SiFAN<sup>+</sup>Br<sup>-</sup> (3)

The preparation of the SiFAN<sup>+</sup>Br<sup>-</sup> (3) started from the SiFA-benzyl alcohol (1), the synthesis of which is described elsewhere [5d]. The reaction of the alcohol 1 with tetrabromomethane [8] gave the corresponding benzylbromide derivative (2) in good yield. The latter was reacted with an excess of N,N-dimethylaminoethanol at 80 °C in a closed vessel (Scheme 1). After evaporation of the excess ethanolamine, compound 3 was obtained as a white and rather hygroscopic solid (m.p. 148 °C) soluble in common polar solvents.

Single crystals of compound 3 suitable for X-ray diffraction analysis were obtained by recrystallization from *n*-hexane/chloroform. The molecular structure of 3 is shown in Fig. 1, selected geometric parameters are collected in Table 1.

Compound 3 crystallizes monoclinically with four molecules in the unit cell. The silicon atom is four-coordinate and shows a distorted tetrahedral configuration. The largest deviations from the tetrahedral angles are found for C(11)-Si-C(15) (119.41(14)°) and F-Si-C(1) (103.95(11)°). The Si-F distance is 1.6051(16) Å and falls into the range of the distances of other SiFA-compounds [5]. A noteworthy feature is the O(1)-H...Br(1) hydrogen bridge (O(1)-H(1) 0.71(3) Å, H(1)...Br(1) 2.52(3) Å, O(1)...Br(1) 3.22(2), ∠O(1)-H(1)-Br(1) 172(4)°) that links the cationic and the anionic part of the compound.

### 2.2. Optimization of the reaction conditions for the isotopic exchange

Based on our previous experience, [<sup>18</sup>F]SiFA building blocks display a high stability at pH ≤ 7.4 found under physiological conditions, but undergo relatively rapid hydrolysis at higher pH. When performing the isotope exchange reaction in dipolar aprotic solvents such as MeCN (Scheme 2), the base used for the azeotropic drying of <sup>18</sup>F<sup>-</sup> as well as its concentration during the isotope exchange reaction appears to have a crucial influence on <sup>18</sup>F incorporation yields despite the absence of water leading to the formation of hydroxide anions. Thus, in order to optimize the incorporation yield of <sup>18</sup>F<sup>-</sup> into 3, the following four parameters were varied: (a) the nature of the base (K<sub>2</sub>CO<sub>3</sub> or K<sub>2</sub>(COO)<sub>2</sub>), (b) the concentration of the base, (c) the amount of 3 and (d) the reaction time of the isotopic exchange. For radio-tracer production, the whole batch of dried <sup>18</sup>F<sup>-</sup> in 0.5–1 mL MeCN, containing μmolar amounts of a base (usually K<sub>2</sub>CO<sub>3</sub>) and Kryptofix 2.2.2 is normally used for the <sup>18</sup>F-radiolabeling reaction. The results show that the yield of the 3/<sup>18</sup>F<sup>-</sup> reaction in MeCN significantly drops when higher amounts of potassium carbonate were used instead of potassium oxalate as a base at a constant amount of the starting material (Fig. 2). Using 10 μg (24 nmol) of 3 and different volumes between 0.2 and 0.7 mL of <sup>18</sup>F<sup>-</sup> (20–50 mCi) from a stock solution of K2.2.2-K<sub>2</sub>C<sub>2</sub>O<sub>4</sub> (27 μmol) in MeCN (2 mL), an almost constant RCY of >90% of [<sup>18</sup>F]3 could be maintained whereas using K2.2.2-K<sub>2</sub>CO<sub>3</sub> stock-volumes of the same concentration (13.5 μmol/mL) of >0.4 mL led to a constant decrease of RCYs (Fig. 2). When 0.7 mL of the stock solution was used, RCYs of only 10% could be obtained with K<sub>2</sub>CO<sub>3</sub> in contrast to 90% when using potassium oxalate.

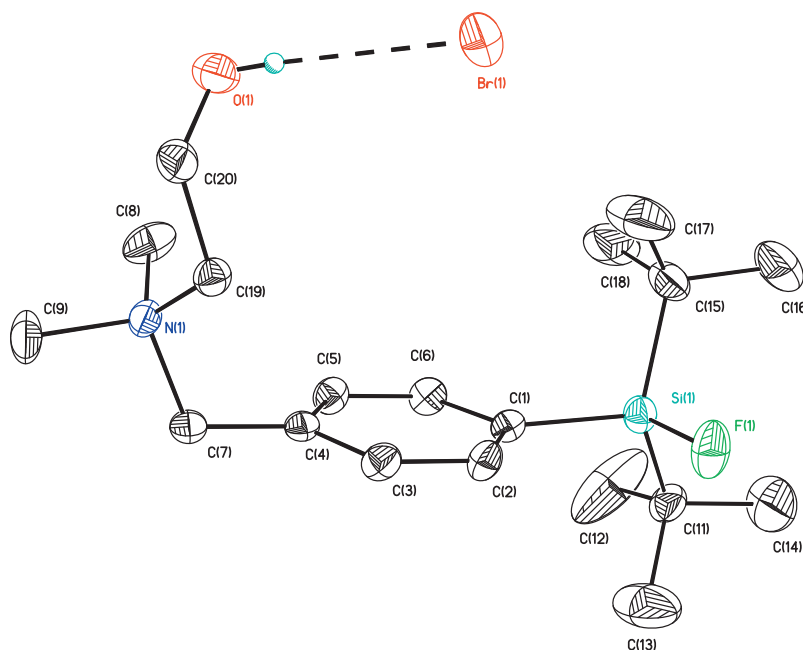


Fig. 1. Molecular structure of **3** measured at 293 K. Atomic displacement parameters are drawn at 30% probability level.

Moreover, using oxalate salt allowed for reducing the amount of the starting material **3** without compromising the RCY of the labeled compound (Fig. 3). In order to maintain RCYs of >50% ( $^{18}\text{F}^-$  incorporation), the amount of the precursor **3** can be kept at as low as 2  $\mu\text{g}$  (5 nmol). The maximum achievable RCY was always reached within 3–5 min upon mixing of the reagents. The azeotropic  $^{18}\text{F}$ -drying process using oxalate was optimized in order to minimize losses of  $^{18}\text{F}^-$  (<10%) during the evaporation steps.

### 2.3. Purification of [ $^{18}\text{F}$ ]SiFAN $^+\text{Br}^-$ ([ $^{18}\text{F}$ ]**3**)

Next, we developed conditions for the purification and final formulation of [ $^{18}\text{F}$ ]**3**. One of the main advantages of [ $^{18}\text{F}$ ]SiFA compounds is their relatively simple purification without HPLC use. Due to very mild reaction conditions no radioactive side-products are usually observed, besides unreacted  $^{18}\text{F}^-$ . As a result of their very different lipophilicities, the separation of [ $^{18}\text{F}$ ]**3** from  $^{18}\text{F}^-$  could be achieved by simple solid phase cartridge extraction. When the crude

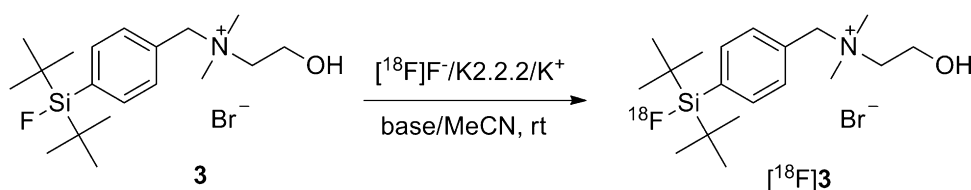
reaction mixture was diluted with water and passed through a C18 cartridge, [ $^{18}\text{F}$ ]**3** was quantitatively retained on the solid phase material whereas the  $^{18}\text{F}^-$  and the Kryptofix 2.2.2. passed through. Interestingly, none of the commonly used organic solvents such as MeOH, MeCN or THF eluted [ $^{18}\text{F}$ ]**3** from the C18 cartridge. However, [ $^{18}\text{F}$ ]**3** was quantitatively recovered using a mixture of MeCN/0.01 M  $\text{H}_3\text{PO}_4$  (4:1). The addition of  $\text{H}_3\text{PO}_4$  enhances the elution strength of the solvent to efficiently elute charged [ $^{18}\text{F}$ ]**3** from the solid phase cartridge. After gentle co-evaporation of the  $\text{H}_3\text{PO}_4/\text{MeOH}$  with ethanol, the residue in the flask appeared to be dry. For the formulation of an injectable solution,  $\text{H}_3\text{PO}_4$  poses no problem since sterile phosphate buffer is added for pH adjustment at the end of synthesis. The radiochemical purity was >99%, as determined by both TLC and HPLC (Fig. 4). In a typical experiment using a starting activity of 1.85 GBq (50 mCi) of  $^{18}\text{F}^-$ , [ $^{18}\text{F}$ ]**3** was obtained in RCYs of 34% (non decay-corrected) after 40 min total preparation time without using HPLC purification.

### 2.4. Specific activity of [ $^{18}\text{F}$ ]**3**

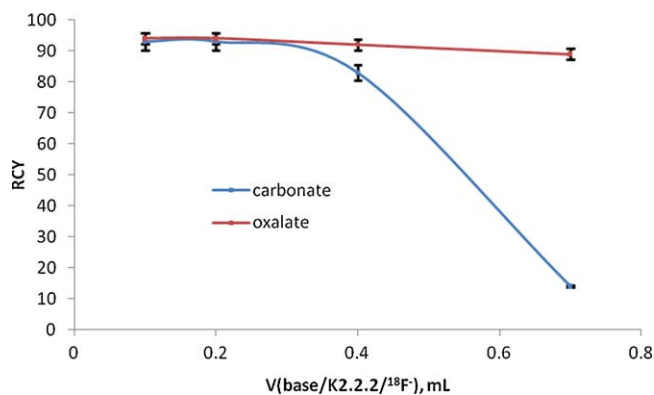
Previously we calculated the SAs of the  $^{18}\text{F}$ -labeled SiFA compounds simply by dividing their radioactivity amount (Ci) by the used amount of SiFA compound ( $\mu\text{mol}$ ). In case of [ $^{18}\text{F}$ ]**3**, we decided to compare the calculated SA with the experimentally determined SA, measured by HPLC chromatography to prove that a simple calculation is sufficient. An aliquot (40  $\mu\text{L}$ ) of purified [ $^{18}\text{F}$ ]**3** from the reaction of 15  $\mu\text{g}$  (36 nmol) **3** and 1.85 GBq (50 mCi)  $^{18}\text{F}^-$  that gave the product in 34% yield was injected into an HPLC system (cf. Section 3). The amount of carrier was determined from the UV calibration curve. The SA of [ $^{18}\text{F}$ ]**3** was precisely calculated

Table 1  
Selected bond lengths [Å] and bond angles [°] for compound **3**.

Bond lengths [Å]		Bond angles [°]	
Si(1)–F(1)	1.6051(16)	F(1)–Si(1)–C(1)	103.95(11)
Si(1)–C(1)	1.862(3)	F(1)–Si(1)–C(11)	104.92(12)
Si(1)–C(11)	1.875(3)	F(1)–Si(1)–C(15)	105.26(12)
Si(1)–C(15)	1.877(3)	C(1)–Si(1)–C(11)	112.55(13)
		C(1)–Si(1)–C(15)	109.22(13)
		C(11)–Si(1)–C(15)	119.41(14)



Scheme 2. Radioactive labeling of **3** via  $^{18}\text{F}$ – $^{19}\text{F}$  isotopic exchange.



**Fig. 2.** Dependence of the incorporation yield of the  $^{18}\text{F}^-$  on the concentration and the kind of the base using a constant amount of the starting material (10  $\mu\text{g}$ , 24 nmol). Using  $\text{K}_2(\text{COO})_2$  the amount of added base has just a minor influence on the RCYs of the isotopic exchange.

knowing the total volume of the product (4.8 mL), its radioactivity (13.3 mCi) and the concentration of non-radioactive **3** (15  $\mu\text{g}$ , 36 nmol) in this aliquot. The experimental value of 0.52 Ci/ $\mu\text{mol}$  closely matched the calculated specific activity of 0.47 Ci/ $\mu\text{mol}$ . Higher specific activities could be easily achievable by increasing the initial activity of  $^{18}\text{F}^-$  and reduction of the starting material **3**, which was limited in our case by radiation safety regulations (of manual manipulations).

### 2.5. Lipophilicity of [ $^{18}\text{F}$ ]**3**

A serious drawback of the SiFA building block comprising two *t*-butyl groups and one benzene moiety is its high lipophilicity. A typical  $\log D$  value, as determined for 4-(di-*tert*-butylfluorosilyl)-benzaldehyde (SiFA-CHO), is 3.6. So far, this has significantly limited possible applications of SiFA compounds for *in vivo* PET imaging. The lipophilicity is less detrimental regarding the labeling of proteins where the SiFA-based labeling synthon imparts only a negligible change onto the protein. [ $^{18}\text{F}$ ]**3**, despite having bulky *t*-butyl and phenyl substituents is a positively charged molecule, containing a hydrophilic quaternary ammonium cation. In order to determine the lipophilicity of [ $^{18}\text{F}$ ]**3**, we measured the partition of purified [ $^{18}\text{F}$ ]**3** between aqueous phosphate buffer (pH 7.4) and octanol-1. The positive charge reduced the overall lipophilicity by a factor of 8 yielding a  $\log D$  value of 0.44.

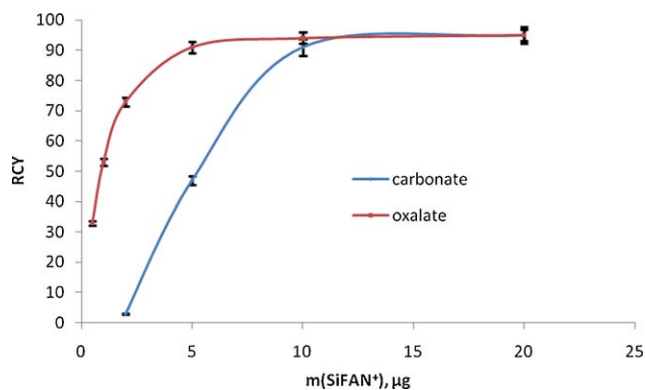


**Fig. 3.** Dependence of the incorporation yield of the  $^{18}\text{F}^-$  on the concentration of the SiFAN<sup>+</sup>Br<sup>-</sup> at a constant concentration of the base ( $2.7 \times 10^{-3}$  M; 0.2 mL from a stock solution (13.5 mmol/L)): (1) carbonate (blue line); (2) oxalate (red line). (For interpretation of the references to color in this figure legend, the reader is referred to the web version of the article.)

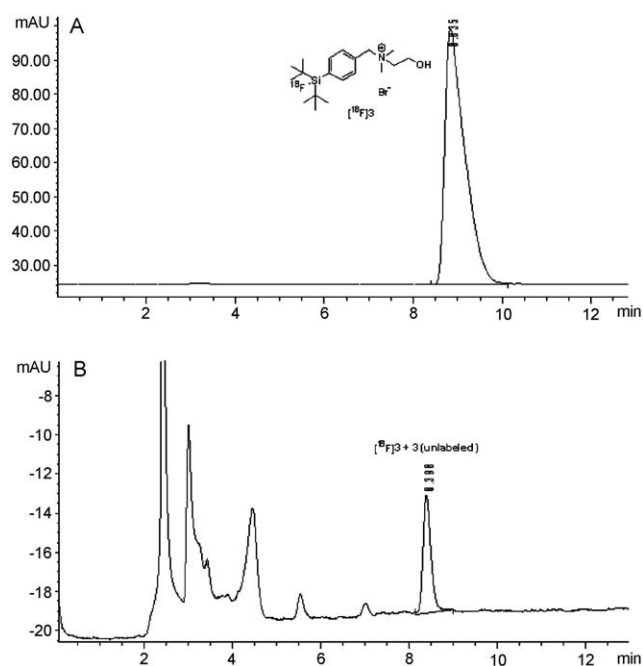


**Fig. 4.** HPLC chromatograms of solid phase purified SiFAN<sup>+</sup>Br<sup>-</sup> [reaction:  $^{18}\text{F}^-$  (1.85 GBq (50 mCi)),  $\text{K}_2.2.2/\text{K}_2(\text{COO})_2$  (13.5  $\mu\text{mol}$ ) in 1 mL MeCN, rt, total synthesis time: 40 min]: (A) radio-HPLC chromatogram, (B) corresponding UV chromatogram.

### 2.6. Hydrolytic stability of [ $^{18}\text{F}$ ]**3**

As expected and in congruence with our previous findings, [ $^{18}\text{F}$ ]**3** was completely stable in acidic media – there is no trace of  $^{18}\text{F}^-$  ions even after 2 h of incubation in aqueous buffer solution at pH 4. In neutral and very slightly basic media (pH 7.0 and 7.4) some hydrolysis was observed but radiochemical impurities did not exceed 5% of the total radioactivity after 2 h. Most importantly, [ $^{18}\text{F}$ ]**3** was found to be very stable in human blood serum upon incubation at 37 °C for 2 h ( $^{18}\text{F}^- \leq 5\%$ ) which is the typical time frame of most *in vivo* PET studies. Increasing hydrolysis over time occurred in stronger basic media (pH 10) – half of [ $^{18}\text{F}$ ]**3** was decomposed after a 2 h incubation time. Kinetic data of the hydrolysis are represented in Fig. 5 as a concentration of free  $^{18}\text{F}^-$  anion versus time at pH 10. The hydrolysis pseudo-first order rate constant was calculated to be  $k' = 1.55 \times 10^{-4} \text{ s}^{-1}$ ,

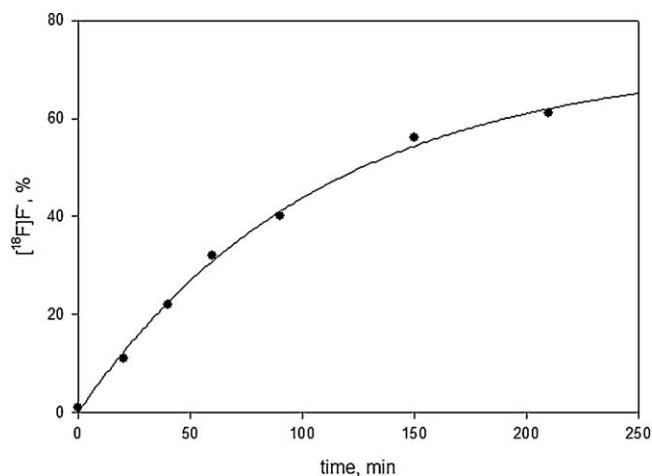


**Fig. 5.** Hydrolysis of [ $^{18}\text{F}$ ]**SiFAN<sup>+</sup>** (ca. 37 MBq (1 mCi) in 1 mL of borate buffer) at pH 10. The appearance of  $^{18}\text{F}^-$  in the solution as a result of hydrolysis is plotted against time.

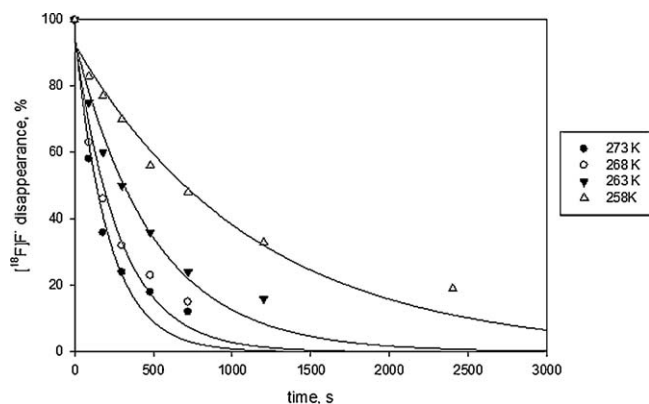


**Fig. 6.** Kinetic curves reflecting the disappearance of  $^{18}\text{F}^-$  during the isotopic exchange reaction in MeCN at different temperatures over time for the determination of the initial rate constants [3: 20  $\mu\text{g}$  (47 nmol); starting activity  $^{18}\text{F}^-$ : 3–5 mCi;  $V_{\text{MeCN}} = 2$  mL].

which corresponds to second order rate constant of  $k = k' / [\text{OH}^-] = 1.55 \text{ L mol}^{-1} \text{ s}^{-1}$  ( $[\text{OH}^-] = 1 \times 10^{-4} \text{ mol L}^{-1}$ ).

### 2.7. Rate constants and activation energy of the isotope exchange reaction

Previously we reported that the high rates of fluorine exchange reaction at the silicon atom are due to the low energy barrier of formation of the penta-coordinated silicon transition state, as confirmed previously by DFT calculations [5]. However, neither isotopic exchange reaction rate constants nor the corresponding activation energy has been previously determined experimentally. In general, these important parameters are very rarely calculated in PET radiochemistry and activation energies of very few  $^{18}\text{F}$ -fluorination reactions have been reported so far [6,9]. In order to determine the Arrhenius preexponential factor and activation energy for the  $^{18}\text{F}$ - $^{19}\text{F}$  isotopic exchange at the silicon atom of compound 3 we decided to carry out a series of experiments at different temperatures. We found experimentally that the optimal temperature range to monitor the labeling of 3 is between  $-20^\circ\text{C}$  and  $0^\circ\text{C}$ , since the reaction is too fast at higher temperatures and too slow at lower temperatures. Concentrations of unlabeled 3 and Kryptofix 2.2.2/ $\text{C}_2\text{O}_4^{2-}/\text{K}^+$  complex in MeCN solutions were kept constant at  $2.38 \times 10^{-4} \text{ M}$  and  $6.7 \times 10^{-3} \text{ M}$ , respectively. The

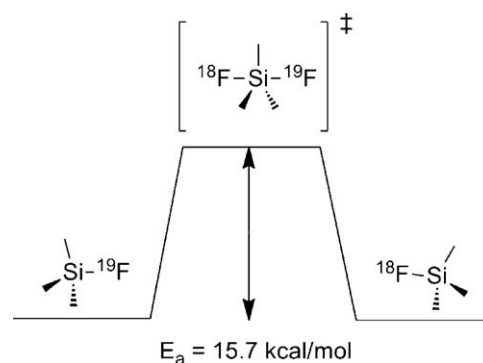


**Fig. 7.** Energy diagram of the  $^{18}\text{F}$ - $^{19}\text{F}$  isotopic exchange reaction ( $\Delta G \approx 0$  because isotope effect is negligibly small). The  $E_a$  of the isotopic exchange reaction was determined to be 15.7 kcal/mol.

added total radioactivity amount of  $^{18}\text{F}^-$  for each experiment was between 111 and 185 MBq (3–5 mCi). The isotopic exchange rate at each individual temperature was monitored by radio-TLC. Fig. 6 shows the resulting kinetic curves of the  $^{18}\text{F}^-$  consumption fitted to an exponential regression, since isotopic exchange is assumed to be a pseudo-first order  $\text{S}_{\text{N}}2$  reaction.

Pseudo-first order initial rate constants at different temperatures were calculated from the exponential fit equation ( $k'_{273} = 4.70 \times 10^{-3} \text{ s}^{-1}$ ;  $k'_{268} = 3.51 \times 10^{-3} \text{ s}^{-1}$ ;  $k'_{263} = 2.01 \times 10^{-3} \text{ s}^{-1}$ ;  $k'_{258} = 8.84 \times 10^{-4} \text{ s}^{-1}$ ) and then divided by concentration of 3 to determine the actual second-order rate constants as follows:  $k_{273} = 19.75 \text{ L mol}^{-1} \text{ s}^{-1}$ ;  $k_{268} = 14.75 \text{ L mol}^{-1} \text{ s}^{-1}$ ;  $k_{263} = 8.45 \text{ L mol}^{-1} \text{ s}^{-1}$ ;  $k_{258} = 3.71 \text{ L mol}^{-1} \text{ s}^{-1}$ .

These rate constants were used to create an Arrhenius plot ( $\ln k$  versus  $T^{-1}$ ) to calculate the activation energy ( $E_a$ ) of the isotope exchange reaction, which was found to be  $65.6 \text{ kJ mol}^{-1}$  (15.7 kcal/mol) (Figs. 7 and 8a). A value of  $7.6 \times 10^{13} \text{ M}^{-1} \text{ s}^{-1}$  was determined for the pre-exponential factor (A). In a comparative study, we determined the activation energy and preexponential values for the  $^{18}\text{F}$ -fluorination of ethyleneglycol-di-*p*-tosylate, an example of conventional  $\text{C}-^{18}\text{F}$  bond formation. This  $^{18}\text{F}$ -fluorination yields one of the most frequently used secondary labeling precursors in radiochemistry [10]. To the best of our knowledge, the kinetic parameters of this benchmark nucleophilic fluorination reaction have never been reported. Rate constants for the fluorination at  $60\text{--}80^\circ\text{C}$  with  $5^\circ\text{C}$  intervals were calculated in the same fashion as

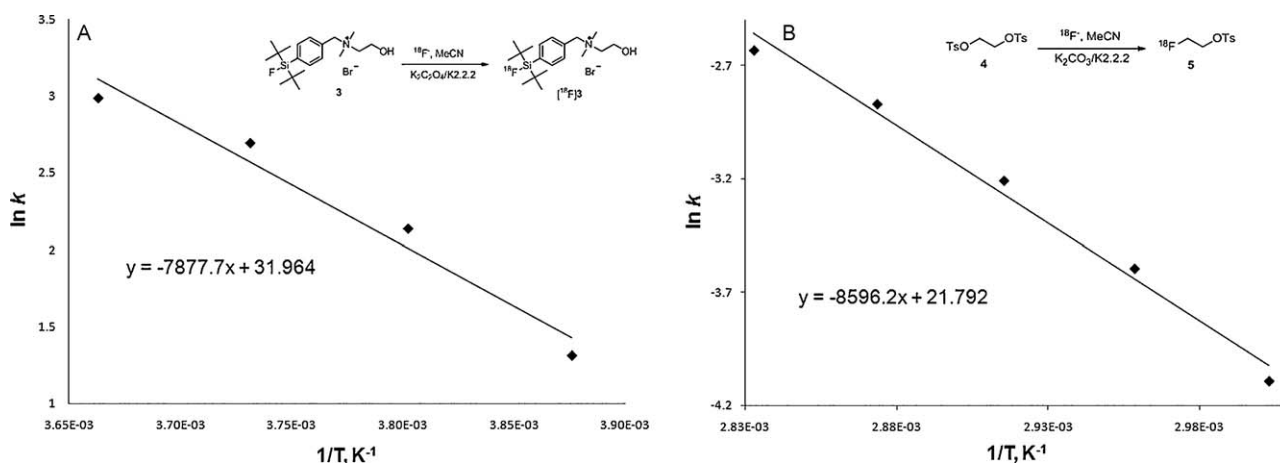


**Fig. 8.** Arrhenius plots of  $\ln k$  against  $1/T$  for (A) the isotopic exchange reaction of 3 with  $^{18}\text{F}^-$  [3: 20  $\mu\text{g}$  (35.7 nmol); starting activity  $^{18}\text{F}^-$ : 110–185 MBq (3–5 mCi);  $V_{\text{MeCN}} = 1$  mL,  $T = -20$  to  $0^\circ\text{C}$ ] and (B) the reaction of ethyleneglycol-di-*p*-tosylate with  $^{18}\text{F}^-$  [ethyleneglycol-di-*p*-tosylate (10 mg, 27  $\mu\text{mol}$ ); starting activity  $^{18}\text{F}^-$ : 110–185 MBq (3–5 mCi);  $V_{\text{MeCN}} = 1$  mL,  $T = 60\text{--}80^\circ\text{C}$ ]. An activation energy of  $65.6 \text{ kJ mol}^{-1}$  (15.7 kcal/mol) and  $71.5 \text{ kJ mol}^{-1}$  (17 kcal/mol) was calculated from plotting  $\ln k$  against  $T^{-1}$  for the isotopic exchange and the fluorination of the tosylate, respectively.



described above and the  $\ln k$  versus  $T^{-1}$  dependence was plotted. The activation energy for this nucleophilic fluorination was found to be  $71.5 \text{ kJ mol}^{-1}$  (17 kcal/mol) (Fig. 8b) which is 1.3 kcal/mol higher than the isotope exchange reaction. The preexponential factor we determined for this reaction was  $2.9 \times 10^9 \text{ M}^{-1} \text{ s}^{-1}$ . The large difference in reactivity for the isotope exchange reaction versus the  $^{18}\text{F}$ -fluorination of ethyleneglycol-di-*p*-tosylate can thus be ascribed to a difference in the preexponential factor, over 4 orders of magnitude larger for the isotope exchange reaction. The smaller (ca. 1.3 kcal) activation energy for the isotope exchange reaction over the  $^{18}\text{F}$ -fluorination of ethyleneglycol-di-*p*-tosylate would also account for the larger rate constant observed for the former over the latter.

### 3. Experimental

#### 3.1. General procedures

Highly enriched [ $^{18}\text{O}$ ]water (>97%) was purchased from Cambridge Isotopes Laboratories. All other commercially available chemicals such as Kryptofix 2.2.2<sup>®</sup>, ethyleneglycol-di-*p*-tosylate, acetonitrile, potassium carbonate and potassium oxalate were of the highest available purity purchased from Sigma-Aldrich. The labeling precursor N-(4-(di-*tert*-butylfluorosilyl)benzyl)-2-hydroxy-N,N-dimethylethylammonium bromide (SiFAN<sup>+</sup>Br<sup>-</sup>, 3) was synthesized as described below. Radio TLCs (silicagel-60 plates) were monitored using an Instant Imager (Packard). Reactions at low temperatures were carried out using a thermostat (FTS Systems). Analytical HPLC was performed on an Agilent Technologies 1200 system equipped with a Gabi radioactivity detector (Raytest). Kinetic experiments were performed using a FTS systems cryostat and the curves were plotted and fitted using Sigma Plot 11.0 software. All solvents used for the syntheses of 1–3 were purified by distillation under argon atmosphere from appropriate drying agents. The NMR experiments were carried out with Bruker DRX 400, Bruker DRX 300 and Varian Mercury 200 spectrometers. The chemical shifts  $\delta$  are given in ppm and are referenced to the solvent peaks with the usual values calibrated against tetramethylsilane ( $^1\text{H}$ ,  $^{13}\text{C}$ ,  $^{29}\text{Si}$ ) and  $\text{CFCl}_3$  ( $^{19}\text{F}$ ). The high resolution mass spectra were obtained with LTQ Orbitrap mass spectrometer (Thermo Electron) using acetonitrile as mobile phase. The acetonitrile solutions were injected via a TriPlus Autosampler onto a DFS-system (Perfluorokerosene as reference), connected with a Trace GC Ultra 2000 system (column: DB-5MS (25 m, 0.25 mm ID, film 0.1  $\mu\text{m}$ )). FT infrared spectra were recorded using a Bruker IFS28 spectrometer. Elemental analyses were performed on a LECO-CHNS-932 analyser.

#### 3.2. X-ray crystallographic procedures

Crystals of compounds 3 (Fig. 1) suitable for single-crystal X-ray diffraction analyses were grown by re-crystallization from  $\text{CHCl}_3/n$ -hexane. Intensity data were collected with a Xcalibur2 CCD diffractometer (Oxford diffraction) with graphite monochromated  $\text{MoK}\alpha$  radiation at 173 K. The data collection covered almost the whole sphere of the reciprocal space with 8 sets at different  $\kappa$  angles and 485 frames by  $\omega$ -rotation ( $\Delta/\omega = 1^\circ$ ) at  $2 \times 40 \text{ s}$  per frame. Crystal decay was monitored by repeating the initial frames at the end of the data collection. After analysis of the duplicate reflections, there was no indication of any decay. The structure was solved by direct methods (SHELXS97) [11]. Refinement applied full-matrix least-squares methods (SHELXL97) [12]. All H atoms were located in the difference Fourier map and their positions were isotropically refined with Uiso constrained at 1.2 times Ueq of the

carrier C atom for non-methyl and 1.5 times Ueq of the carrier C atom for methyl groups. Atomic scattering factors for neutral atoms and real and imaginary dispersion terms were taken from International Tables for X-ray Crystallography [13]. The figure was created by SHELXTL [14]. Crystallographic data for the structure reported in this paper have been deposited by the Cambridge Crystallographic Data Centre as supplementary material publication no. CCDC-790848. Copy of the data can be obtained free of charge on application to CCDC, 12 Union Road, Cambridge, CB2 1EZ, UK (fax: +44 1223 336033, e mail: deposit@ccdc.cam.ac.uk).

#### 3.3. Synthesis of the [4-(di-*tert*-butylfluorosilyl)benzyl]-(2-hydroxyethyl)-dimethylammonium bromide, SiFAN<sup>+</sup>Br<sup>-</sup> (3)

##### 3.3.1. (4-Bromomethylphenyl)-di-*tert*-butyl-fluorosilane (2)

To a  $0^\circ\text{C}$  cooled solution of the SiFA-benzyl alcohol 1 (3.08 g, 11.5 mmol) and tetrabromomethane (4.18 g, 12.6 mmol, 1.1 equiv.) in 100 mL dichloromethane triphenylphosphine (3.30 g, 12.6 mmol, 1.1 equiv.) was added over a period of 30 min in small portions [8]. The solution was stirred for 2 h at room temperature and turned yellow during this time. The solvent was removed *in vacuo* and the residue was washed with cold *n*-hexane (150 mL). The white precipitate was removed by filtration, the clear solution was concentrated *in vacuo* and purified by column chromatography ( $\text{SiO}_2$ , 100% pentane). Compound 2 was isolated as a colorless oil (3.06 g, 9.2 mmol, 80%), which solidified on standing (m.p.  $52^\circ\text{C}$ ).

$^1\text{H}$  NMR (400.13 MHz,  $\text{CDCl}_3$ ):  $\delta$  7.58 (d,  $^3J(^1\text{H}-^1\text{H}) = 8 \text{ Hz}$ , 2H,  $\text{H}_m$ ), 7.40 (d,  $^3J(^1\text{H}-^1\text{H}) = 8 \text{ Hz}$ , 2H,  $\text{H}_o$ ), 4.49 (s, 2H,  $\text{CH}_2$ ), 1.05 (s, 18H,  $\text{Si}(\text{C}(\text{CH}_3)_3)_2$ ).

$^{13}\text{C}\{^1\text{H}\}$  NMR (100.63 MHz,  $\text{CDCl}_3$ ):  $\delta$  138.8 (d,  $^3J(^{13}\text{C}-^{19}\text{F}) = 14 \text{ Hz}$ ,  $\text{C}_p$ ), 134.4 (d,  $^3J(^{13}\text{C}-^{19}\text{F}) = 4 \text{ Hz}$ ,  $\text{C}_m$ ), 128.1 (s,  $\text{C}_o$ ), 125.9 (s,  $\text{C}_i$ ), 27.2 (s,  $\text{Si}(\text{C}(\text{CH}_3)_3)_2$ ), 20.2 (d,  $^2J(^{13}\text{C}-^{19}\text{F}) = 12 \text{ Hz}$ ,  $\text{Si}(\text{C}(\text{CH}_3)_3)_2$ ).

$^{19}\text{F}$  NMR (282.38 MHz,  $\text{CDCl}_3$ ):  $\delta$  188.9 (s,  $^1J(^{19}\text{F}-^{29}\text{Si}) = 299 \text{ Hz}$ ).

$^{29}\text{Si}\{^1\text{H}\}$  NMR (59.63 MHz,  $\text{CDCl}_3$ ):  $\delta$  14.3 (d,  $^1J(^{29}\text{Si}-^{19}\text{F}) = 299 \text{ Hz}$ ).

Elemental analyses: calculated (%) for  $\text{C}_{15}\text{H}_{24}\text{FSiBr}$  (331.34 g/mol) C 54.4, H 7.3, found C 54.4, H 7.6.

HR-GC-ESI-MS: calculated ( $m/z$ ) for  $\text{C}_{15}\text{H}_{24}\text{F}^{28}\text{Si}^{79}\text{Br}^+$  330.0815, found 330.0814.

##### 3.3.2. SiFAN<sup>+</sup>Br<sup>-</sup> (3)

A mixture of the SiFA-benzyl bromide 2 (0.57 g, 1.72 mmol) and N,N-dimethyl ethanolamine (0.78 g, 1 mL, 8.81 mmol) was heated for 24 h at  $80^\circ\text{C}$  in a glass vessel with a Teflon valve (F. Young). The excess of ethanolamine was removed *in vacuo* and the ammonium salt was re-crystallized from  $\text{CHCl}_3/n$ -hexane. Compound 3 (0.41 g, 0.97 mmol, 56%) was obtained as colorless crystals (m.p.  $148^\circ\text{C}$ ).

$^1\text{H}$  NMR (400.13 MHz,  $\text{CDCl}_3$ ):  $\delta$  7.65 (s, 4H,  $\text{H}_{arom}$ ), 5.12 (t,  $^3J(^1\text{H}-^1\text{H}) = 5 \text{ Hz}$ , 1H, OH), 4.92 (s, 2H,  $\text{PhCH}_2$ ), 4.22 (m, 2H,  $\text{NCH}_2$ ), 3.81 (m, 2H,  $\text{CH}_2\text{OH}$ ), 3.32 (s, 6H,  $\text{NCH}_3$ ), 0.99 (s, 18H,  $\text{Si}(\text{C}(\text{CH}_3)_3)_2$ ).

$^{13}\text{C}\{^1\text{H}\}$  NMR (100.63 MHz,  $\text{CDCl}_3$ ):  $\delta$  137.4 (d,  $^3J(^{13}\text{C}-^{19}\text{F}) = 14 \text{ Hz}$ ,  $\text{C}_p$ ), 134.6 (d,  $^3J(^{13}\text{C}-^{19}\text{F}) = 4 \text{ Hz}$ ,  $\text{C}_m$ ), 132.3 (s,  $\text{C}_o$ ), 128.3 (s,  $\text{C}_i$ ), 68.6 (s,  $\text{PhCH}_2$ ), 65.9 (s,  $\text{NCH}_2$ ), 55.9 (s,  $\text{CH}_2\text{OH}$ ), 50.8 (s,  $\text{NCH}_3$ ), 27.2 (s,  $\text{Si}(\text{C}(\text{CH}_3)_3)_2$ ), 20.1 (d,  $^2J(^{13}\text{C}-^{19}\text{F}) = 12 \text{ Hz}$ ,  $\text{Si}(\text{C}(\text{CH}_3)_3)_2$ ).

$^{19}\text{F}$  NMR (282.38 MHz,  $\text{CDCl}_3$ ):  $\delta$  187.8 (s,  $^1J(^{19}\text{F}-^{29}\text{Si}) = 299 \text{ Hz}$ ).

$^{29}\text{Si}\{^1\text{H}\}$  NMR (59.63 MHz,  $\text{CDCl}_3$ ):  $\delta$  13.7 (d,  $^1J(^{29}\text{Si}-^{19}\text{F}) = 299 \text{ Hz}$ ).

Elemental analyses: calculated (%) for  $\text{C}_{19}\text{H}_{35}\text{FNOSiBr}$  (420.48 g/mol) C 54.3, H 8.4, N 3.3, found C 52.3, H 8.5, N 3.4.

HR-LC-ESI-MS: calculated ( $m/z$ ) for  $\text{C}_{19}\text{H}_{35}\text{FNO}^{28}\text{Si}^+$  340.2466, found 340.2466.

### 3.4. Radiochemistry

#### 3.4.1. Azeotropic drying of $^{18}\text{F}^-$

No-carrier-added (nca)  $^{18}\text{F}^-$  was generated by the bombardment of an enriched [ $^{18}\text{O}$ ]water target (>97%, 2.2 mL) with a proton beam (35  $\mu\text{A}$ ) using an IBA cyclotron (Cyclon 18/9) for 10 min. The resulting aqueous [ $^{18}\text{F}$ ]F $^-$ /H $_2$ [ $^{18}\text{O}$ ]O (3.7–7.4 GBq; 100–200 mCi) was transferred to a hot cell and passed through a preconditioned (10 mL 0.5 M K $_2$ CO $_3$  followed by 10 mL deionized water) QMA SepPak Light cartridge (Waters). The H $_2$ [ $^{18}\text{O}$ ]O was collected and the fixed  $^{18}\text{F}^-$  was eluted from the QMA cartridge with a solution of Kryptofix 2.2.2 $^{\text{®}}$  (10 mg), either 0.25 M K $_2$ CO $_3$  (60  $\mu\text{L}$ ) or 0.25 M K $_2$ C $_2$ O $_4$  (60  $\mu\text{L}$ ) and MeCN (1 mL). The solvents were removed under a gentle vacuum of ca. 500 mbar and a sweep stream of argon at 90  $^{\circ}\text{C}$ . The remaining traces of water were removed by azeotropic co-evaporation with MeCN (1 mL) twice. After all the solvents were visibly removed the argon flow was stopped, the vacuum was set to maximum (ca. 10 mbar) and the final drying was continued for 2 min.

#### 3.4.2. $^{18}\text{F}$ -labeling of 3 via isotopic exchange at room temperature

In order to optimize the reaction conditions, the dried [ $^{18}\text{F}$ ]F $^-$ /Kryptofix 2.2.2 $^{\text{®}}$ /K $^+$  complex was re-dissolved in 1 mL of acetonitrile. Aliquots of this solution were mixed at room temperature with aliquots of a stock solution of precursor 3 ( $c = 1 \mu\text{g}/\mu\text{L}$ ), investigated amount of 3: 1–800  $\mu\text{g}$ ) in anhydrous MeCN in Eppendorf vials (1.5 mL). Each reaction mixture was kept at room temperature and was analyzed by TLC (CH $_2$ Cl $_2$ /MeOH/ACOH 7:2:1, R $_f = 0.5$ ) at different time points (3–50 min) and the  $^{18}\text{F}^-$  incorporation yield was determined as percentage of the radioactivity of the spot corresponding to [ $^{18}\text{F}$ ]3 to the total radioactivity of the TLC plate (only two spots were detectable: [ $^{18}\text{F}$ ]3 + unreacted  $^{18}\text{F}^-$ ). To separate the labeled product from unreacted  $^{18}\text{F}^-$ , the crude reaction mixture was diluted with water (10 $\times$  the volume of the crude reaction mixture) and the resulting solution was passed through a preconditioned (10 mL MeOH followed by 10 mL of water) C-18 light cartridge (SepPak, Waters). The cartridge was washed with 10 mL water to remove all traces of residual  $^{18}\text{F}^-$  and Kryptofix 2.2.2 $^{\text{®}}$ . The desired [ $^{18}\text{F}$ ]3 was nearly quantitatively (>97%) eluted from the cartridge with MeOH/0.01 M H $_3$ PO $_4$  (2 mL, 4:1). Both aqueous and organic eluates were analyzed by means of radio-TLC using the conditions reported above to confirm the quantitative separation of unreacted  $^{18}\text{F}^-$  anion and [ $^{18}\text{F}$ ]3. The product was collected in a round-bottom flask and the solvent was removed by evaporation using a water bath at gentle heat ( $\leq 70 \text{ }^{\circ}\text{C}$ ) and a vacuum of 20 mbar. Higher temperatures led to a decomposition of [ $^{18}\text{F}$ ]3. Ethanol (100%, 2 mL) was then added and the solution was re-evaporated in order to remove all traces of methanol and H $_3$ PO $_4$ . Finally, [ $^{18}\text{F}$ ]3 was re-dissolved in ethanol (0.3 mL) and sterile phosphate buffer (2.7 mL) for the final formulation. It could be shown that the compound did not decompose under these conditions mimicking an injectable solution for animal or human PET experiments.

#### 3.4.3. Synthesis of [ $^{18}\text{F}$ ]3 at a higher MBq (mCi) level

We applied the optimized isotopic exchange reaction conditions to synthesize a large radioactivity amount of [ $^{18}\text{F}$ ]3 and calculate the overall preparative radiochemical yield of the product. 1.85 GBq (50 mCi)  $^{18}\text{F}^-$  was fixed on the QMA cartridge and eluted with a mixture of Kryptofix 2.2.2 (5 mg, 13.3  $\mu\text{mol}$ ) and K $_2$ C $_2$ O $_4$  (6.7  $\mu\text{mol}$ ) in acetonitrile/water (95:5, V = 2 mL). The resulting complex was dried as described above (a slightly lower vacuum was applied to keep losses of  $^{18}\text{F}^-$  during the drying below 10%) and 3 (15  $\mu\text{g}$ , 35.7 nmol) was added from a stock solution (1  $\mu\text{g}/\mu\text{L}$ ) in anhydrous MeCN (1 mL). The reaction mixture was kept at room temperature for 5 min (incorporation yield of  $^{18}\text{F}^-$

was  $\sim 50\%$  as determined by TLC) then quenched with water (20 mL), and purified on a C18 cartridge as described above. [ $^{18}\text{F}$ ]3 (492–629 MBq (13.3–17 mCi), radiochemical purity >99%) was dissolved in EtOH (0.5 mL) and sterile phosphate buffer (4.5 mL).

#### 3.4.4. Determination of specific activity (SA) of [ $^{18}\text{F}$ ]3

To determine the SA of [ $^{18}\text{F}$ ]3, a small aliquot (40  $\mu\text{L}$ ) of the aforementioned solution (cf. Section 3.4.3) was analyzed by means of radio-HPLC using a Prodigy ODS (5  $\mu\text{m}$ , 250 mm  $\times$  4.6 mm) column (Phenomenex) and acetonitrile/20 mM KH $_2$ PO $_4$  (55:45) as a mobile phase (flow rate: 1 mL/min). A calibration curve (UV detection at 230 nm) to calculate the amount of 3 was created by injecting solutions of unlabeled 3 of different concentrations (1, 2, 5 and 10  $\mu\text{g}/\text{mL}$ ). The retention time of 3 at a flow rate of 0.8 mL/min was 8.8 min (Fig. 4).

#### 3.4.5. Determination of the lipophilicity of [ $^{18}\text{F}$ ]3

In order to determine the log  $D$  value, the dried [ $^{18}\text{F}$ ]3 (ca. 37 MBq (1 mCi)) was dissolved in phosphate buffer (pH 7.4) and an aliquot of this solution (0.5 mL) was placed into an Eppendorf tube. Octanol-1 (0.5 mL) was added and the mixture was vigorously shaken using a Vortex apparatus for 5 min. After centrifugation (14,500 rpm, 3 min), the aqueous and organic phases were carefully separated and their radioactivity content measured in a calibrated curimeter. The experiment was done in triplicate and the ratio of the total radioactivities of the two phases was used to calculate the log  $D$ . In addition to this procedure and to corroborate the results, equal volumes (1  $\mu\text{L}$ ) from each phase were spotted on a TLC plate and the ratio of the activities was determined with an Instant Imager (Packard Canberra). The calculated log  $D$  values using these two different methods matched and were averaged over three experiments for each method.

#### 3.4.6. Stability of [ $^{18}\text{F}$ ]3 towards hydrolysis at different pH

[ $^{18}\text{F}$ ]3 was synthesized and purified as described above and then re-dissolved in aqueous methanol (10%, 2 mL). Equal aliquots (300  $\mu\text{L}$ , ca. 1 mCi) of the resulting solution were diluted with standard commercially available aqueous buffers of known pH (700  $\mu\text{L}$ , pH 4, 7, 7.4 and 10) at room temperature and with human blood serum (1 mL, pH 7.4) at 37  $^{\circ}\text{C}$ . Each solution was analyzed by radio-TLC for up to 4 h by taking small aliquots at different time points (20–240 min) to determine the concentration of unbound  $^{18}\text{F}^-$ . For the experiment at pH 10, the amount of unbound  $^{18}\text{F}^-$  was plotted versus time to calculate a hydrolysis rate constant.

#### 3.4.7. Rate constants of isotopic exchange and Arrhenius plot

3.4.7.1. [ $^{18}\text{F}$ ]3. To determine the rate constants and activation energy ( $E_a$ ), the  $^{18}\text{F}^-$ / $^{19}\text{F}$  isotope exchange reaction between 3 and  $^{18}\text{F}^-$  was monitored at four different temperatures (0  $^{\circ}\text{C}$ ,  $-5 \text{ }^{\circ}\text{C}$ ,  $-10 \text{ }^{\circ}\text{C}$ , and  $-15 \text{ }^{\circ}\text{C}$ ) using equal amounts of the precursor (20  $\mu\text{g}$ , 47 nmol) and  $^{18}\text{F}^-$ /Kryptofix 2.2.2 $^{\text{®}}$ /oxalate/K $^+$  complex (3–5 mCi). Each reaction was monitored by radio-TLC at several time points up to 40 min. The radioactivity amount corresponding to  $^{18}\text{F}^-$  was plotted versus time to calculate the isotope exchange pseudo-first order rate constants at different temperatures. The resulting data were used to create an Arrhenius plot (ln  $k$  versus  $1/T$ ) to calculate the corresponding preexponential factor and the activation energy of the isotope exchange from the slope of the plot.

3.4.7.2. Nucleophilic fluorination of ethyleneglycol-di- $p$ -tosylate. Aliquots of ethyleneglycol-di- $p$ -tosylate solution in MeCN (2.7  $\mu\text{mol}$  in 100  $\mu\text{L}$ ) were added to the stock solution of the [ $^{18}\text{F}$ ]F $^-$ /Kryptofix 2.2.2 $^{\text{®}}$ /oxalate/K $^+$  (100  $\mu\text{L}$  3–5 mCi) complex in Eppendorf tubes and reaction mixtures were heated up to 60–80  $^{\circ}\text{C}$  in 5  $^{\circ}\text{C}$  increments and monitored by radio-TLC at certain time-

points. The rate constants were determined in the same fashion as described above for the  $[^{18}\text{F}]\mathbf{3}$  and were used to create an Arrhenius plot to calculate the preexponential factor and the activation energy of this nucleophilic substitution from the slope of the plot.

#### 4. Conclusions

We demonstrated that charged SiFA compounds such as N-(4-(di-*tert*-butyl $[^{18}\text{F}]$ fluorosilyl)benzyl)-2-hydroxy-N,N-dimethylethylammonium bromide ( $[^{18}\text{F}]\text{SiFAN}^+\text{Br}^-$ ,  $[^{18}\text{F}]\mathbf{3}$ ) can be obtained in high RCYs at low temperatures via simple isotope exchange with SAs between 400 and 550 Ci/mmol. The salt  $[^{18}\text{F}]\mathbf{3}$  was purified by simple solid phase cartridge extraction and isolated in high RCY of 27–34% (uncorrected for radioactive decay) in as little as 40 min.  $[^{18}\text{F}]\mathbf{3}$  was proven to be 8-times more hydrophilic ( $\log D = 0.44$ ) than previously reported SiFA compounds and stable in aqueous buffers up to pH 7.4. The compound was also found to be stable in human serum at 37 °C for 2 h. The isotope exchange reaction was characterized to be very fast even below room temperature (–20 °C) and a relatively high Arrhenius preexponential factor of  $7.6 \times 10^{13} \text{ M}^{-1} \text{ s}^{-1}$  and low activation energy of 65.6 kJ mol $^{-1}$  (15.7 kcal/mol) were experimentally determined from the corresponding Arrhenius plot. The formation of a carbon– $^{18}\text{F}$  bond via nucleophilic substitution using ethyleneglycol-di-*p*-tosylate as a labeling precursor yielded a 1.3 kcal/mol higher activation energy and a much lower preexponential factor of  $2.9 \times 10^9 \text{ M}^{-1} \text{ s}^{-1}$  making the isotopic exchange reaction kinetically more favorable. Charged  $[^{18}\text{F}]\text{SiFA}$  compounds have the potential to become valuable new labeling synthons for the development of SiFA-based  $^{18}\text{F}$ -fluorinated radiopharmaceuticals. Especially peptide and protein labeling will benefit from the development of hydrophilic SiFA building blocks. We are currently in the process of synthesizing additional SiFAN $^+$  derivatives bearing a thio- or amino group instead of the relatively un-reactive hydroxy moiety. These compounds are intended for subsequent bioconjugation to maleimido-derivatized peptides and proteins by click chemistry.

#### References

[1] K. Hamacher, H.H. Coenen, G. Stöcklin, J. Nucl. Med. 27 (1986) 235–238.

- [2] (a) D. Le Bars, J. Fluorine Chem. 127 (2006) 1488–1493;  
 (b) R. Schirmmayer, C. Wängler, E. Schirmmayer, Mini Rev. Org. Chem. 4 (2007) 317–329;  
 (c) H.J. Wester, M. Schottelius, in: P.A. Schubiger, L. Lehmann, M. Friebe (Eds.), PET Chemistry – The Driving Force in Molecular Imaging, 2006, 79–111;  
 (d) L. Chai, S.Y. Lu, V.W. Pike, Eur. J. Org. Chem. 17 (2008) 2853–2873;  
 (e) P.W. Miller, N.J. Long, R. Vilar, A.D. Gee, Angew. Chem. Int. Ed. 47 (2008) 8998–9033;  
 (f) S.M. Ametamey, M. Honer, P.A. Schubiger, Chem. Rev. 108 (2008) 1501–1506;  
 (g) Wängler C., Schirmmayer R., Bartenstein P., Wängler B., Curr. Med. Chem. 17 (2010) 1092–1116.
- [3] (a) J. Becaud, L. Mu, M. Karramkam, P.A. Schubiger, S.M. Ametamey, K. Graham, T. Stellfeld, L. Lehmann, S. Borkowski, D. Berndorff, L. Dinkelborg, A. Srinivasan, B. Koks, Bioconjugate Chem. 20 (2009) 2254–2261;  
 (b) U. Roehn, J. Becaud, L. Mu, A. Srinivasan, T. Stellfeld, A. Fitzner, K. Graham, L. Dinkelborg, A.P. Schubiger, S.M. Ametamey, J. Fluorine Chem. 130 (2009) 902–912.
- [4] (a) M.S. Rosenthal, A.L. Bosch, R.J. Nickles, S.J. Gately, Int. J. Appl. Radiat. Isot. 48 (1985) 318–319;  
 (b) A.R. Studenov, M.J. Adam, J.S. Wilson, T. Ruth, J. Labelled Compd. Radiopharm. 48 (2005) 497–500;  
 (c) R. Ting, M.J. Adam, T.J. Ruth, D.M. Perrin, J. Am. Chem. Soc. 127 (2005) 13094–13095;  
 (d) L.J. Mu, A. Hoehne, P.A. Schubiger, S.M. Ametamey, K. Graham, J.E. Cyr, L. Dinkelborg, T. Stellfeld, A. Srinivasan, U. Voigtmann, U. Klar, Angew. Chem. Int. Ed. 47 (2008) 4922–4925;  
 (e) P. Laverman, W.J. McBride, R.M. Sharkey, A. Eek, L. Joosten, W.J.G. Oyen, D.M. Goldberg, O. Boerman, J. Nucl. Med. 51 (2010) 454–460.
- [5] (a) R. Schirmmayer, G. Brandtmöller, E. Schirmmayer, O. Thews, J. Tillmanns, T. Siessmeier, H.G. Buchholz, P. Bartenstein, B. Wängler, C.M. Niemeyer, K. Jurkschat, Angew. Chem. Int. Ed. 45 (2006) 6047–6050;  
 (b) E. Schirmmayer, B. Wängler, M. Cypriak, G. Brandtmöller, M. Schäfer, M. Eisenhut, K. Jurkschat, R. Schirmmayer, Bioconjugate Chem. 18 (2007) 2085–2089;  
 (c) B. Wängler, G. Quandt, L. Iovkova, E. Schirmmayer, C. Wängler, G. Boening, M. Hacker, M. Schmoekel, K. Jurkschat, P. Bartenstein, R. Schirmmayer, Bioconjugate Chem. 20 (2009) 317–321;  
 (d) L. Iovkova, B. Wängler, E. Schirmmayer, R. Schirmmayer, G. Quandt, G. Boening, M. Schürmann, K. Jurkschat, Chem. Eur. J. 15 (2009) 2140–2147.
- [6] F. Cacace, M. Speranza, A.P. Wolf, R.R. MacGregor, J. Fluorine Chem. 21 (1982) 145–158.
- [7] A. Hoehne, L. Mu, M. Honer, P.A. Schubiger, S.M. Ametamey, K. Graham, T. Stellfeld, S. Borowski, D. Berndorff, U. Klar, U. Voigtmann, J.E. Cyr, M. Friebe, L. Dinkelborg, A. Srinivasan, Bioconjugate Chem. 19 (2008) 1871–1879.
- [8] A. Ianni, S.R. Waldvogel, Synthesis 13 (2006) 2103–2112.
- [9] J.-H. Chun, S. Lu, Y.-S. Lee, V.W. Pike, J. Org. Chem. 75 (2010) 3332–3338.
- [10] D. Block, H.H. Coenen, G. Stöcklin, J. Labelled Compd. Radiopharm. 25 (1987) 201–216.
- [11] G.M. Sheldrick, Acta Crystallogr. A46 (1996) 467.
- [12] G.M. Sheldrick, University Goettingen, 1991.
- [13] International Tables for Crystallography, 1992, Vol. C, Dordrecht: Kluwer Academic Publishers.
- [14] G.M. Sheldrick, 1997, SHELXTL Release 5.1 Software Reference Manual, Bruker AXS, Inc., Madison, Wisconsin, USA.